In: Paparoditis N., Pierrot-Deseilligny M., Mallet C., Tournaire O. (Eds), IAPRS, Vol. XXXVIII, Part 3A – Saint-Mandé, France, September 1-3, 2010

Contents   Keyword index   Author index

QUALITY MEASURE FOR TEXTURES EXTRACTED FROM AIRBORNE IR IMAGE SEQUENCES

D. Iwaszczuk, U. Stilla

Photogrammetry and Remote Sensing, Technische Universitaet Muenchen (TUM) - (iwaszczuk, stilla)@bv.tum.de

Commission III, WG III/5

KEY WORDS: Infrared Images, Image Sequences, Automated Texture Mapping, 3D Building Models, Oblique View

ABSTRACT: Energy and climate changes are big topics in near future. In the European countries a significant part of consumed energy is used for heating in the buildings. Much effort is required for reducing this energy loss. Inspection and monitoring of buildings contribute in further development saving energy. For detection of areas with the highest loss of heat thermal infrared (IR) imaging can be used. For such inspection a spatial correspondence between IR-images and existing 3D building models is helpful. This correspondence can be created by geo-referencing of the images. Then, the 3D model can be projected into the image and for each surface of the model a region of the image can be selected for texture. In this paper a concept for the texture mapping using IR image sequences is introduced. Emphasis is placed on analysis of texture quality and resolution changes in oblique view images. The influence of the angular aperture and inclination angle on the effective texture resolution is discussed. A formula for calculation of texture quality is proposed. For experiments with data an IR image sequence of test area "Technische Universitet Muenchen" in Munich is used.

1. INTRODUCTION

1.1 Motivation

Due to the climate changes and increasing energy costs became the energy efficiency an important topic. In the European countries 40 % of the energy is consumed by buildings, whereas 47% is used for heating. Much effort is required for reducing the energy loss. Inspection and monitoring of buildings contribute in further development saving energy. Thermal infrared (IR) imaging can be used to detect areas with highest loss of heat. Nowadays usually single IR images are analyzed, without reference to the geometry of the captured scene, often manually. It does not allow a combination of thermal data with other imagery or semantic information stored in a spatial data base, is time consuming and not applicable for large areas. For geo-referencing the IR images can be combined with three-dimensional geometry of the buildings as textures and in these textures heat leakages can be detected (Hoegner & Stilla, 2009). Such monitoring of whole cities allows creation of an open geographic information systems (GIS), where citizens could view the energy loss of their houses.

High resolution, terrestrial IR images can be acquired using a mobile platform and used for texturing of façades (Hoegner & Stilla, 2007). However, these images do not capture the roofs and façades from inner yards or building rings. To complete the coverage of the buildings with textures oblique view images from an airborne platform can be used (Grenzdoerffer et al., 2008; Stilla et al., 2009; Kolecki et al., 2010).

1.2 Related work

In recent years the process of automatic texture mapping has been frequently discussed within photogrammetry and computer vision. The major problems connected to the automation of the texturing are:
- geo-referencing,
- self-calibration of the camera,
- automatic visibility checking and self occlusions,
- elimination of extrinsic occlusions,
- selection of the best image for the texture from an available set of images.

For geo-referencing of aerial images, the exterior orientation (ExtOri) parameters of the camera are needed. Approximated, but stable position and orientation of the sensor can be directly determined using global positioning system (GPS). An inertial navigation system (INS) provides good short-term accuracy, but in a longer time a systematic drift occurs. Thus, the combination of GPS and INS allows to avoid the INS drift and to bridge any loss of satellite signal by GPS (Yastikli & Jacobsen, 2005). Unfortunately, often the camera position and orientation are not identical with position and orientation registered by GPS/INS device. In that case the estimation of the misalignment angles (boresight parameters) and the lever arm vector is necessary (E Yastikli & Jacobsen, 2005; Eugster & Nebiker, 2007; Stilla et al., 2009; Kolecki et al., 2010). Furthermore, most of building models are stored in national coordinates, while GPS/INS navigation uses geographic coordinate system. Skaloud & Legat (2008) present necessary transformations between both coordinate systems.

However, the accuracy of direct geo-referencing is not appropriate for a precise texture mapping with high-resolution images. Additionally, the interior orientation parameters are usually only approximately known. Therefore a self-calibration algorithm is required. Frueh et al. (2004) proposes an approach based on matching of line segments with model edges. In this method the edges are extracted in the image and the model is projected into the image from a random pose of the camera. For this pose a rating based on line matching is calculated and this procedure is repeated. The pose with the highest rating is chosen for texture mapping. However, computational effort of this method is very high. Ding & Zakhor (2008) present an algorithm for self-calibration divided in two steps. In the first step vanishing points corresponding to vertical lines and GPS-

In: Paparoditis N., Pierrot-Deseilligny M., Mallet C., Tournaire O. (Eds), IAPRS, Vol. XXXVIII, Part 3A – Saint-Mandé, France, September 1-3, 2010

Contents   Keyword index   Author index

data are used to estimate an approximated camera position. In the second step 2D points in the image are extracted and matched with 3D points of the model using Hough transform and generalized M-estimator. Then the Lowe's (1987) algorithm is applied for refinement of the camera parameters. This approach yields very good results for in downtown area; however, it fails at residential region because of not enough extracted vertical edges.

In texture mapping using thermal images the properties specific to the IR spectrum should be taken into consideration. First of all, IR images have lower contrast and lower resolution than images in visible spectrum. Consequently, matching with 3D building model based on edge matching (Frueh et al., 2004) or on vertical vanishing points (Ding & Zakhor, 2008) could be difficult. Stilla et al. (2000) proposed a method for matching of low resolution IR images based on intersection points of roof edges.

For texture mapping a visibility analysis is necessary. Generally, there are two groups of methods for checking of the visibility: (i) variations of depth-buffer (depth image) approach (Frueh et al., 2004; Hoegner & Stilla, 2007; Karras et al., 2007) and (ii) polygon-based hidden area detection (Kuzmin et al., 2004). In the polygon-based method proposed by Kuzmin et al. (2004) all polygons are projected onto image plane and intersected. This procedure is appropriate for nadir view images, because of small number of intersections. However, using oblique view this method would be very time consuming and could cause many small polygons.

The depth-buffer method is a basic method removing hidden surfaces adopted from computer graphics. The depth-buffer is a matrix storing for every pixel the distance from projection centre to the model surface. This method was often proposed in some variations. Karras et al. (2007) tries to generalize the problem of orthorectification and texture mapping. He proposes a method for visibility checking based on depth image. Every triangulated 3D mesh is projected onto projection plane and for every triangle occupied pixels get identity number (ID) of the triangle. For pixels with more IDs the closest one is chosen. Frueh et al. (2004) used a modified depth-buffer storing additionally the product of a triangle's normal vector with the camera viewing direction at each pixel. Using information about vector product not occluded edges can be detected. Abdelhafiz & Niemeier (2009) integrate digital images and laser scanning point clouds. They use a Multi Layer 3GImage algorithm which classifies the visibility on two stages: point stage and surface stage. The visible layer and back layers are applied. Occluded vertexes are sent to a back layer, while visible vertexes appear on the visible layer. An image is used for texture mapping of a mesh, if all three vertexes of it are visible in this image.

Abdelhafiz & Niemeier discuss also the problem of extrinsic (un-modelled) occlusions caused by such objects as traffic signs, trees and street-lamps. They propose a Photo Occlusion Finder algorithm which checks textures from many images for one mesh. When the textures of one mesh are not similar an occlusion occurred.

Objects taken by image sequences with a high frame rate from a flying platform appear in multiple frames. In this case textures with optimal quality have to be taken for texturing. Lorenz & Doellner (2006) introduced a local effective resolution and discuss it on example of images from a High Resolution Stereo Camera (HRSC) due to its special projection of line scanners

(perspective and parallel). Frueh et al. (2004) uses a focal plane array. He determines optimal textures taking into account occlusion, image resolution, surface normal orientation and coherence with neighbouring triangles. He proposes to accept textures with few occluded pixels instead textures with very low resolution taken from extremely oblique view. This quality calculation is focused on texturing with optical images and good user perception.

In this paper we propose a texture selection method for thermal inspection of buildings using a weighted quality function. This approach allows reducing or increasing the influence of occlusions, distance and viewing directions on the texture quality. In Chapter 2 a necessary for texturing camera calibration, positioning and orientation is described. In chapter 3 a concept for texture mapping is introduced. Moreover, the influence of oblique view imagery on texture resolution is discussed. The equation for weighted quality measure is presented. Finally, in Chapter 4 experiments with some exemplary textures are shown and discussed in chapter 5.

2. SYSTEM CALIBRATION

In most cases, how already mentioned, GPS/INS data do not refer to the projection centre. Consequently, boresight and leverarm parameters are required. In addition, camera parameters, such as focal length, principle point, and distortions, need to be determined. As the solution we propose a system calibration using an extended bundle adjustment with camera self calibration which is described by Kolecki et al. (2010). In this method in few images of the sequence ground control points (GCP) need to be measured and all parameters of exterior and interior orientation as well as boresight and leverarm corrections should be estimated. Parameters obtained in the adjustment should be applied for projection onto all images of the sequence.

3. A CONCEPT FOR TEXTURE MAPPING

The region within an IR frame corresponding to a face of the 3D model can be determined by projection of the polygons into the image. In datasets captured by moving cameras with high frame rate most polygons of the model appear many times in the images with different aspect angles. This advantage allows choosing the texture captured from the best pose. Additionally in some cases and bridge the problem of occlusions can be resolved. The quality of the textures extracted from different frames belonging to the same plane varies depending on viewing direction, distance to the camera, and partial occlusions. For selecting the best texture a quality measure has to be defined and the selection procedure has to be implemented. A flowchart of this procedure is depicted in Fig. 1.

Starting from the first frame for each face a projection is carried out. If the face lies within the frame a partial occlusion o_{ij} (Chapter 3.1) and quality measure q_{ij} (Chapter 3.3) are calculated. In case that the quality q_{ij} of is higher than the quality of the currently stored texture, new texture t_{ij} is created and the current texture is overwrite with t_{ij}.

3.1 Occlusions

Every face is projected into the image and pixels occupied by this plane get the ID of this plane and its distance from the projection centre. A pixel is considered as occupied if its centre

In: Paparoditis N., Pierrot-Deseilligny M., Mallet C., Tournaire O. (Eds), IAPRS, Vol. XXXVIII, Part 3A – Saint-Mandé, France, September 1-3, 2010

Contents | Keyword index | Author index

lies inside of plane polygon. If a pixel has assigned more than one ID, the closer plane is marked as visible. Based on this image it is possible to determine for each plane the fraction o_i of occlusion as follows:

$$o_{ij} = \frac{n}{N} \qquad (1)$$

where:

n – number of occluded pixels in plane i,
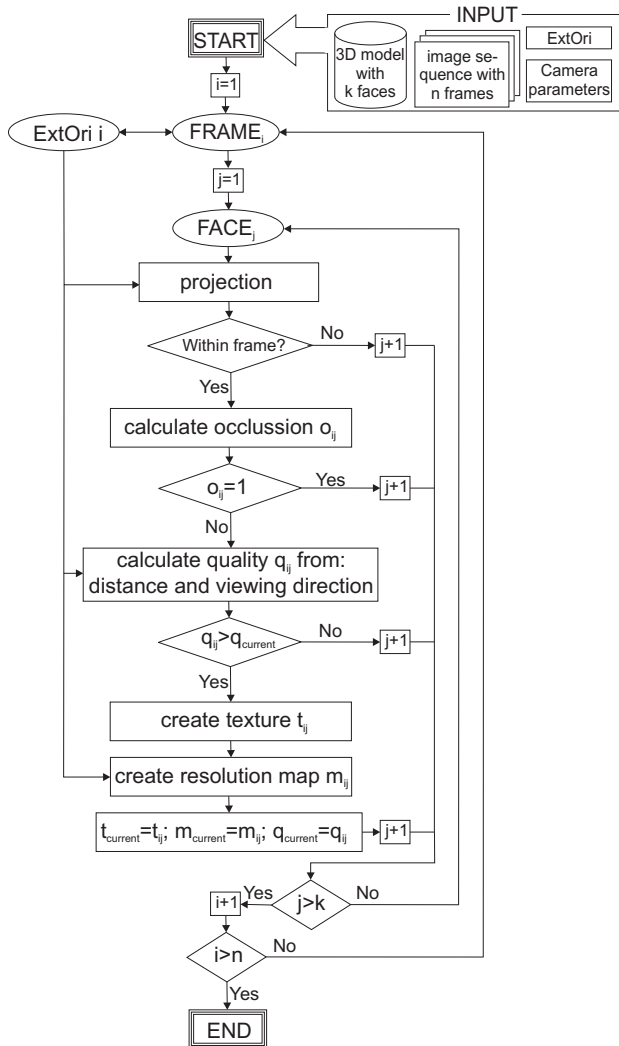N – number of pixels occupied by plane i.

Figure 1. A concept for texture mapping using texture qualities

3.2 Texture resolution

In nadir view the ground resolution of the images, usually expressed in ground sample distance (GSD), depends on aircraft altitude, digital terrain model and pixel size. Using oblique view the ground resolution depends also on the image coordinates. More specifically, objects situated at near range have higher resolution than objects at the same height seen at far range. In consequence, even horizontal faces don't have an unique resolution. For storing the original resolution of the texture its resolution map need to be created. This original resolution of the texture depends on orientation of the face and the distance from the camera. In the Fig. 2 a situation is shown where the face (roof) is seen in far and near range.
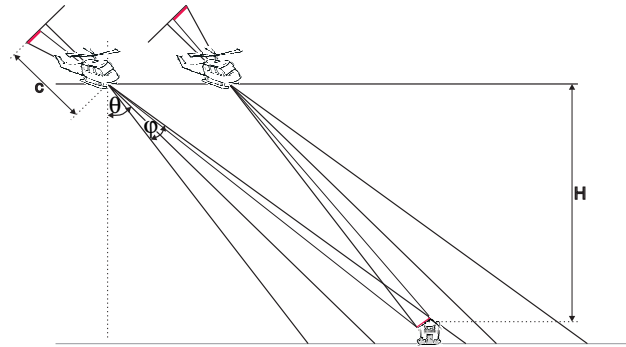

Figure 2. Image acquisition with oblique view

We assume that this roof is a differential surface, is always oriented to the camera and the aircraft has a linear trajectory. In this way the changes in the resolution between far and near range can be investigated. The projection of this surface onto image plane is depicted in Fig. 3.
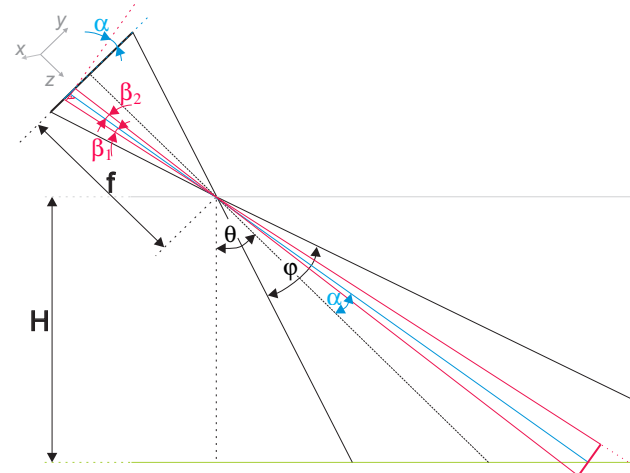

Figure 3. Projection of a differential surface oriented to the projection centre

The angles β1 and β2 can be calculated by equation (2).

$$\beta_1 = arctg(tg\,\alpha - \frac{pp}{2f}) - \alpha \qquad \beta_2 = \alpha - arctg(tg\,\alpha + \frac{pp}{2f}) \qquad (2)$$

where:

pp – pixel pitch
f – focal length

Therefore, the resolution of the differential surface along y-axis in camera coordinate system can be calculated as follows:

$$r(y) = \frac{\cos(\theta + \alpha_y)}{H \cdot (tg\beta_{1y} + tg\beta_{2y})}[pixel/m] \qquad (3)$$

$$\alpha_y \in \left[-\frac{\varphi}{2}, \frac{\varphi}{2}\right]$$

where:

$r(y)$ –resolution of the along y-axis
H – aircraft altitude above the differential plane
θ – inclination angle (pitch angle)
φ – angular aperture

Analogical, the resolution along x-axis can be calculated using equations (4).

In: Paparoditis N., Pierrot-Deseilligny M., Mallet C., Tournaire O. (Eds), IAPRS, Vol. XXXVIII, Part 3A – Saint-Mandé, France, September 1-3, 2010

Contents   Keyword index   Author index

$$r(x) = \frac{\cos(\alpha_x)}{H \cdot (tg\beta_{1x} + tg\beta_{2x})} [pixel/m] \qquad (4)$$

$$\alpha_x \in \left[-\frac{\varphi}{2}, \frac{\varphi}{2} \right]$$

Depending on this both angles the change of resolution between the far and close range of the image can be calculated as factor η expressed by equation (5).

$$\eta = \frac{r_n(y) - r_f(y)}{r_f(y)} \qquad (5)$$

where:

r_n – ground resolution at near range
r_f – ground resolution at far range

Different values of p for different cameras and different viewing angle are presented in table 1.

| Camera: | φ[°] | θ=25 ° | θ=35 ° | θ= 45° | θ=55 ° |
		η	η	η	η
PCE-TC 2	20	0.18	0.28	0.43	0.67
Flir A325	25	0.23	0.37	0.57	0.93
PCE-TC 2	32	0.31	0.50	0.80	1.39

Table 1. Changes of the resolution between near and far range of an orthogonally oriented surface depending on inclination angle and camera type (angular aperture)

For description of planes which are seen under angle $\gamma \neq 90°$ the equations (3) and (4) can be extended as follows:

$$r(y) = \frac{\cos(\theta + \alpha_y) \cdot \cos(\gamma_x)}{H \cdot (tg\beta_{1y} + tg\beta_{2y})}$$

$$r(x) = \frac{\cos(\alpha_x) \cdot \cos(\gamma_x)}{H \cdot (tg\beta_{1x} + tg\beta_{2x})} \qquad (6)$$

where:

γ_x, γ_y – angles between normal of the plane and the viewing direction of the camera on the respectively xz-plane and yz-plane in camera coordinate system

Using equations (5) and (6) the changes of resolution of a differential surface which is seen in far range from angle $\gamma_f \rightarrow 90°$ can be calculated. Then in the near range $\gamma_n = \gamma_f - \varphi$.

| Camera: | φ[°] | θ=25 ° | θ=35 ° | θ= 45° | θ=55 ° |
		η	η	η	η
PCE-TC 2	20	4.72	5.22	5.93	7.11
Flir A325	25	6.06	6.85	8.01	10.05
PCE-TC 2	32	8.04	9.37	11.46	15.48

Table 2. Changes of the resolution between near and far range of a surface seen from angle γ close to 90°

Comparing Tables 1 and 2 can be assessed that for surfaces seen from an angle close to 90° the change of the distance is not significant, while for surfaces seen from an extremely unfavourable angle the difference between far and near range is meaningful.

Due to rasterisation each texture is an image which has an equal-distance sampling. The gray values of the texture need to be calculated from the original IR image. For preserving the original resolution the grid for the texture has to be designed with maximal resolution which can occur.

For definition of the best possible resolution two strategies can be considered:

- Every plane in the model gets the same ground resolution. The advantage of this strategy is that already at the beginning of the texturing process all texture matrixes can be predefined and the memory necessary to store the textures can be planed. A homogeneous ground resolution of the textures is also advantageous during image analysis, such as feature extraction, because the scale of the detected features is the same for all textures. On the other hand, in this method many textures synthetically get much higher resolution then it was in the original image. Consequently, more memory is consumed as necessary.

- The best possible resolution is determined separately for every plane. Specifically, for every plane in every image the point with the best resolution is found and the resolution of this point is applied for the texture creation.

The best possible resolution can be calculated assuming that it occurs at orthogonally oriented differential surface placed in one of the points of the 3D model. Based on ExtOri parameters for first frame of the sequence and the resolution in all visible points can be calculated with the equation (3). The best resolution is stored. Then the same procedure can be applied for other frames. If a higher resolution was found, the value is overwritten.

3.3 Texture quality

For optimal texture selection a quality measure q_i of every texture should be calculated as follows:

$$q_{ij} = \frac{a_1 \cdot (1 - o_{ij}) + a_2 \cdot d_{ij} + a_3 \cdot \cos\gamma_{xij} \cdot \cos\gamma_{yij}}{a_1 + a_2 + a_3} \qquad (7)$$

$$a_1 + a_2 + a_3 \neq 0$$

where:

γ_x, γ_y – angles between normal of a model polygon and viewing angle of the camera,
a_1, a_2, a_3 – coefficients,
o_i – occlusion factor,
d_i – distance factor – calculated by equation (8).

$$d_{ij} = \frac{D_{max} - D_{ij}}{D_{max} - D_{min}} \qquad (8)$$

where:

D_{max} – maximal possible distance from the projection centre to model points,
D_{min} – minimal possible distance from the projection centre to model points,
D_i – distance from the projection centre to the centre of a model polygon.

In general textures with high occlusion shouldn't be considered in texturing process. In case of small occlusion, the occluded part can be replaced by parts of textures with lower resolution. The balance between occlusion factor and other factors can be set using coefficients a_1, a_2 and a_3. In case of object recognition, for instance windows, from textures a higher resolution is preferred. Thus the coefficient a_1 should be smaller

In: Paparoditis N., Pierrot-Deseilligny M., Mallet C., Tournaire O. (Eds), IAPRS, Vol. XXXVIII, Part 3A – Saint-Mandé, France, September 1-3, 2010

Contents   Keyword index   Author index

than in case of thermal inspection of the buildings, where radiometry of the texture is very important. Before combining a texture from more images the changes of radiometry in whole sequence should be investigated. If they are remarkable the textures should be extracted from one image only, even with lower resolution. Radiometric adjustment of the texture from multiple images in case of thermal inspection shouldn't be applied at all.

Although the distance factor (d) and surface orientation angles (χ_x, χ_y) in the quality equation reflect the effective resolution of texture, they should be considered separately. When the angles χ_x, χ_y are large, the resolution of the texture is not only low, but also inhomogeneous. For avoiding this situation the coefficient a_3 should be set higher then a_2.

4. EXPERIMENTS

4.1 Data overview

During the flight campaign a helicopter flew four times above the test area TUM recording a sequence of oblique images. This dataset was taken additionally and simultaneously to a laser scanning during a flight campaign (Hebel & Stilla, 2007). Afterwards four subsequences (stripes #1, #2, #3 and #4) representing each of the four flights were cut out. The helicopter trajectory and the stripes' directions are shown in Fig. 4. The intersection of the trajectory is located above the centre of the test area.

Figure 4. Flight trajectory over test area TUM (Hebel & Stilla 2007)

The inclination angle of the optical axis is approximately 45°. Images were captured with the AIM 640 QLW FLIR infrared camera with the frame rate of 25 images per second. The image resolution is 640 x 512 pixels.

4.2 Results

For presentation of the proposed quality measure some exemplary textures with different qualities ware extracted (Figures 5, 6 and 7). The quality measures $q_{ij-1} - q_{ij-3}$ were calculated with a choice of coefficients a_1, a_2 and a_3.

a)

$\chi_x=0°$ $\chi_y=33°$ $d_{ij}=0,20$ $q_{ij-1}=0,68$ frame 2003, #1
$q_{ij-2}=0,74$
$q_{ij-3}=0,48$

b)

$\chi_x=0°$ $\chi_y=25°$ $d_{ij}=0,73$ $q_{ij-1}=0,88$ frame 2128, #1
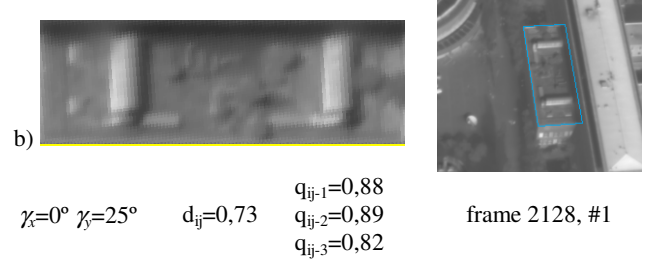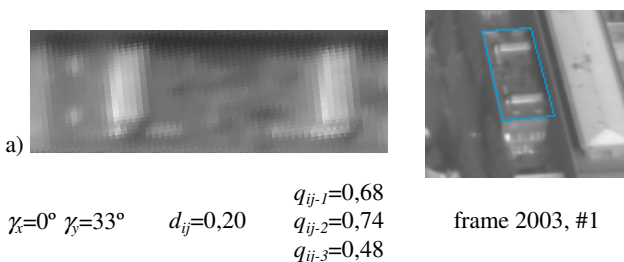$q_{ij-2}=0,89$
$q_{ij-3}=0,82$

Figure 5. Textures of the same roof with different quality factors. q_{ij-1} was calculated with $a_1=a_2=a_3=1$; q_{ij-2} with $a_1=a_2=1$ and $a_3=3$; q_{ij-3} with $a_1=a_3=1$ and $a_2=3$

a)

$\chi_x=1°$ $\chi_y=30°$ $d_{ij}=0,17$ $q_{ij-1}=0,68$ frame 2018, #1
$q_{ij-2}=0,75$
$q_{ij-3}=0,47$

b)

$\chi_x=1°$ $\chi_y=32°$ $d_{ij}=0,52$ $q_{ij-1}=0,79$ frame 2128, #1
$q_{ij-2}=0,81$
$q_{ij-3}=0,68$

c)

$\chi_x=84°$ $\chi_y=1°$ $d_{ij}=0,62$ $q_{ij-1}=0,58$ frame 13267, #4
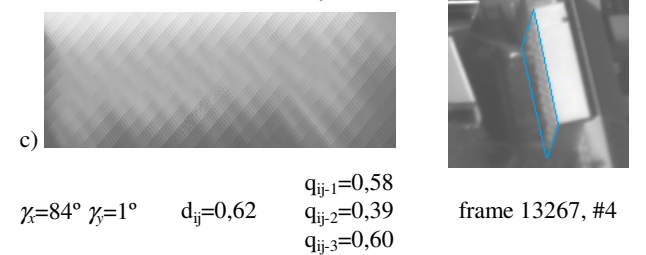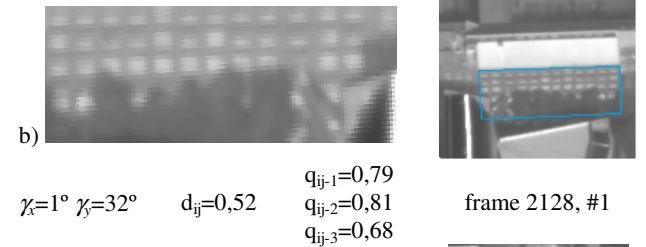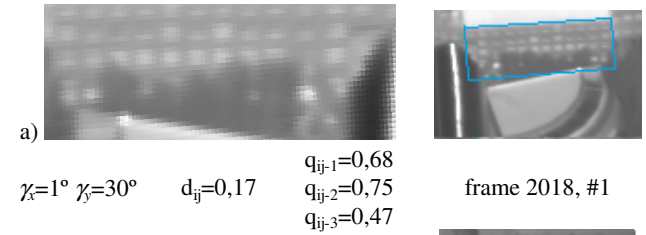$q_{ij-2}=0,39$
$q_{ij-3}=0,60$

Figure 6. Textures of the same wall with different quality factors and from different stripes. For q_{ij-1}, q_{ij-2}, q_{ij-3} – see Fig. 5
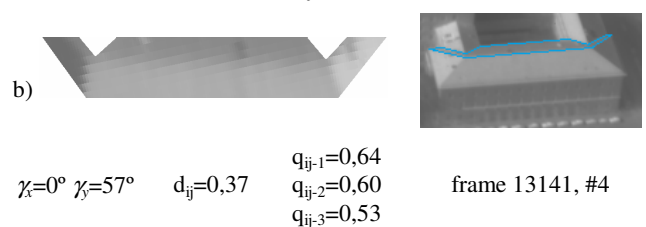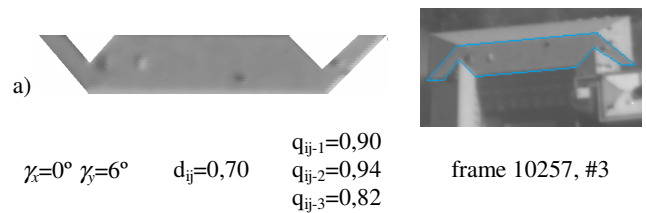

a)

$\chi_x=0°$ $\chi_y=6°$ $d_{ij}=0,70$ $q_{ij-1}=0,90$ frame 10257, #3
$q_{ij-2}=0,94$
$q_{ij-3}=0,82$

b)

$\chi_x=0°$ $\chi_y=57°$ $d_{ij}=0,37$ $q_{ij-1}=0,64$ frame 13141, #4
$q_{ij-2}=0,60$
$q_{ij-3}=0,53$

Figure 7. Textures of the same roof from different stripes. For q_{ij-1}, q_{ij-2}, q_{ij-3} – see Fig. 5

5. DISCUSSION

The main part of the concept presented in this paper consists of texture selection using weighted quality measure. The introduced equation for calculating the quality q allows reducing and increasing of the influence of particular component, such as distance, occlusion and viewing direction.

On the examples from the Chapter 4.2 can be observed, that the large viewing angle makes the texture unreadable. Furthermore, often in such textures the difference in resolution along x and y axis is significant. To avoid this effect which is disrupting for observer, the influence of the viewing direction should be increased. For this reason the weight a_3 in the equation (7) should be set higher than a_1 and a_2. It can be noticed that the results for q_{ij-2} are intuitively better than for q_{ij-1} and q_{ij-3}.

Comparing textures from Fig. 6a and 7b having the almost equal quality q_{ij-1} by $a_3=a_2$ can be noticed, that the wall texture (Fig. 6a) is much more useful than the roof surface from Fig. 7b. Considering the quality q_{ij-2} where $a_3>a_2$ we see that the quality of the wall texture has significantly higher value which correspond to our perception.

In Fig. 7b we can also observe mismatch between image and the projected model, which is especially remarkable by narrow polygons seen under large angle. As result of a disadvantageous orientation the texture depicted in the Fig. 6c is completely useless for object extraction, which is also represented in q_{ij-2} better than in q_{ij-1} and q_{ij-3}.

REFERENCES

Abdelhafiz A, Niemeier W (2009), In: Godhoff F, Staiger R. Terrestrisches Laserscanning (TLS 2009). Yes, we Scan! Beiträge zum 91. DVW-Seminar am 19. und 20. November 2009 in Fulda. Schriftreihe eds DVW. Band 60/2009

Ding M, Zakhor A (2008) Automatic registration of aerial imagery with untextured 3D LiDAR models, IEEE Computer Society Conference on Computer Vision and Pattern Recognition (CVPR), Anchorage, Alaska, June 2008

Eugster H., Nebiker S. (2007) Geo-registration of Video Sequences Captured from Mini UAVs – Approaches and Accuracy Assessment, 5th International Symposium on Mobile Mapping Technology - Padua, Italy

Frueh C, Sammon R, Zakhor A (2004) Automated Texture Mapping of 3D City Models With Oblique Aerial Imagery. In: Proceedings of the 2nd International Symposium on 3D Data Processing, Visualization, and Transmission (3DPVT'04)

Grenzdoerffer, J.G., Guretzki M., Friedlander I. (2008) Photogrammetric Image Acquisition and Image Analysis of Oblique Imagery. In: The Photogrammetric Record, 23(124): 372–386

Hebel M., Stilla U. (2007) Automatic registration of laser point clouds of urban areas. In: Stilla U, Meyer H, Rottensteiner F, Heipke C, Hinz S (eds) PIA07 - Photogrammetric Image Analysis 2007. International Archives of Photogrammetry, Remote Sensing and Spatial Information Sciences, Vol. 36 (3/W49A): 13-18

Hoegner L, Stilla U (2007) Automated generation of 3D points and building textures from infrared image sequences with ray casting. In: Stilla U, Meyer H, Rottensteiner F, Heipke C, Hinz S (eds) PIA07 - Photogrammetric Image Analysis 2007. International Archives of Photogrammetry, Remote Sensing and Spatial Information Sciences, Vol 36(3/W49B):65-70

Hoegner L, Stilla U (2009) Thermal leakage detection on building facades using infrared textures generated by mobile mapping. Joint Urban Remote Sensing Event (JURSE 2009). IEEE

Karras G, Grammatikopoulos L, Kalisperakis I, Petsa E (2007) Generation of Orthoimages and Perspective Views with Automatic Visibility Checking and Texture Blending. Photogrammetric Engineering & Remote Sensing, Vol. 73, No. 4, April 2007: 403-411

Kolecki J, Iwaszczuk D, Stila U (2010) Calibration of an IR camera system for automatic texturing of 3D building models by direct geo-referenced images. Calibration and Orientation Workshop EuroCOW 2010. Castelldefels, Spain

Kuzmin Y P, Korytnik S A, Long O (2004) Polygon-based true orthophoto generation, International Archives of Photogrammetry, Remote Sensing and Spatial Information Sciences, 35 (Part 3): 529-531

Lorenz H, Doellner J (2006) Facade Texture Quality Estimation for Aerial Photography in 3D City Models, Meeting of the ICA commission on Visualization and Virtual Environments, Vancouver, Canada

Lowe D G (1987) Three-dimensional object recognition from single two-dimensional images. Artificial Intelligence, 31(3): 355–395.

Skaloud J, Legat K (2008), Theory and reality of direct geo-referencing in national coordinates. In: ISPRS Journal of Photogrammetry and Remote Sensing, Vol. 63, Issue 2, March 2008: 272-282

Stilla U, Kolecki J, Hoegner L (2009) Texture mapping of 3D building models with oblique direct geo-referenced airborne IR image sequences. ISPRS Hannover Workshop 2009: High-Resolution Earth Imaging for Geospatial Information. International Archives of Photogrammetry, Remote Sensing and Spatial Information Sciences 38(1-4-7/W5) (on CD ROM)

Stilla U, Sörgel U, Jäger K (2000) Generation of 3D-city models and their utilisation in image sequences. International Archives of Photogrammetry and Remote Sensing. Vol. 33, Part B2: 518-524

ACKNOWLEADGMENTS